JPE 16-2-23

http://dx.doi.org/10.6113/JPE.2016.16.2.631
ISSN(Print): 1598-2092 / ISSN(Online): 2093-4718

The Influence of Changing PV Array Interconnections under a Non-uniform Irradiance

Kun Ding†, Li Feng*, Si-Yu Qin*, Jing Mao**, Jing-Wei Zhang*, Xiang Wang*, Tao Peng*, and Quan-Xin Zhai***

†,*College of Mechanical and Electrical Engineering, Hohai University, Jiangsu, China
**State Key Laboratory of PV Science and Technology, Jiangsu, China
***Changzhou Key Laboratory of Photovoltaic System Integration and Production Equipment Technology, Jiangsu, China

Abstract

Usually, the output characteristics of a photovoltaic (PV) array are significantly affected by non-uniform irradiance which is caused by ambient obstacles, clouds, orientations, tilts, etc. Some local maximum power points (LMPP) in the current-voltage (I-V) curves of a PV array can result in power losses of the array. However, the output power at the global maximum power point (GMPP) is different in different interconnection schemes in a PV array. Therefore, based on the theoretical analysis and mathematical derivation of different topological structures of a PV array, this paper investigated the output characteristics of dual series PV arrays with different interconnections. The proposed mathematical models were also validated by experimental results. Finally, this paper also concluded that in terms of performance, the total cross tied (TCT) interconnection was not always the optimal structure, especially in a dual series PV array. When one of the PV modules was severely mismatched, the TCT worked worse than the series parallel (SP) structure. This research can provide guidance for switching the interconnection to gain the greatest energy yield in a changeable- structure PV system.

Key words: Experiment, Interconnection schemes, Non-uniform irradiance, Photovoltaic (PV) array, Simulation

I. INTRODUCTION

Due to the decreasing supply of traditional fossil fuels and global warming, photovoltaic (PV) power has been widely used as a form of sustainable energy in recent decades. However, because outdoor-installed PV modules cannot achieve the same performance as those in a laboratory, the operating conditions of a PV array should be taken into careful consideration. As shown in previous studies [1]-[5], the presence of non-uniform irradiance, such as the shadows of surrounding obstacles, clouds, bird droppings, orientation or tilt can result in mismatching losses of a PV array. A PV array made up of PV modules connected in series can be regarded as a PV string. When the short-circuit current of shaded PV modules is less than the operating current of a PV string, the bypass diodes of the shaded PV modules are conducted and the multiple power peak phenomenon of the I-V curve will occur.

Some published papers reported methods for alleviating the influence of a non-uniform irradiance by changing the PV array interconnections [6]-[8]. Three main topology structures have been designed for PV arrays: the series parallel (SP), bridge link (BL) and total cross tied (TCT) structures, as shown in Fig. 1. In the SP topology, PV strings are not interconnected. However, they are entirely interconnected on each row of junctions in the TCT topology. In the BL topology, PV strings are interconnected alternatively. A common conclusion is that the TCT topology is the most efficient interconnection structure for reducing the loss of generated power under the same conditions [9]. In other words, more interconnections can generate more power in a PV array under non-uniform irradiance conditions. In paper [9], in order to improve the output power of a PV array, the reasons why the TCT and BL configurations are superior to the SP configuration were discussed. Interconnected PV strings can mitigate the influence

Manuscript received May. 3, 2015; accepted Aug. 31, 2015
Recommended for publication by Associate Editor Hyung-Min Ryu.
†Corresponding Author: dingkunhhu@163.com
Tel: +86-519-85191952, Fax: +86-519-85120010, Hohai University
*College of Mechanical and Electrical Eng., Hohai University, China
**State Key Laboratory of PV Science and Technology, China
***Changzhou Key Laboratory of Photovoltaic System Integration and Production Equipment Technology, China

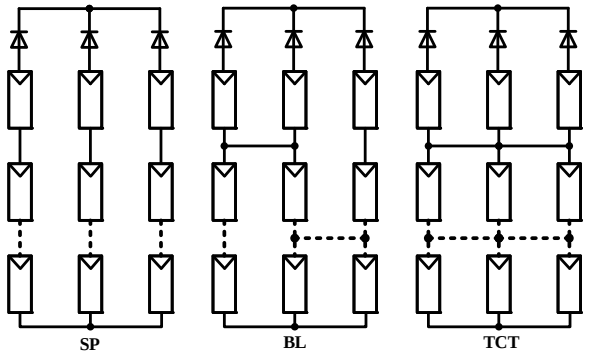

Fig. 1. Different topology structures of a PV array.

of the shaded PV modules in the series-connected branch where the shaded PV modules are located.

Nevertheless, these papers [6-7] analyzed the distinctions of different PV array interconnections only with experimental results, rather than theoretically analyzing the operation process of PV arrays, i.e. obtaining power at the MPP through mathematical derivation.

Therefore, this paper studied the performance of different PV array interconnections under the conditions of non-uniform irradiance. It also presents a theoretical analysis and experimental results. Firstly, a 3×2 PV array with only one shaded PV module was discussed. Then, the performances of the interconnection structures in dual and triple series connected PV systems were investigated. The results indicate that the TCT structure is not always the optimal topology structure for maximizing the output power in a mismatched PV array. The performance of different structures in a PV array is significantly influenced by the mismatch level of the shaded PV module and the shadow location.

II. ANALYSIS OF PV ARRAY TOPOLOGY STRUCTURES

In order to analyze the output performance of each interconnection structure for a PV array with only one shaded PV module, the relationship between the mismatch level and the output power of each structure should be investigated. In this section, the healthy PV modules are assumed to operate under the standard test condition (STC) and the mismatch severity is evaluated based on the level of equivalent irradiance of the shaded PV module. Hence, mathematical equations are deduced to describe the relationship between the level of irradiance of the shaded module and the output power of different PV array structures. The 3×2 PV array, which is formed by 3 rows and 2 columns of PV modules, is discussed first due to its simplicity in terms of deduction and calculation.

A. Model of a PV Module

A solar cell is usually represented by single-diode or two-diode models. Due to the simplicity and accuracy of the single-diode model [10], [11], it is used in this paper, and its equivalent circuit is shown in Fig. 2 [12].

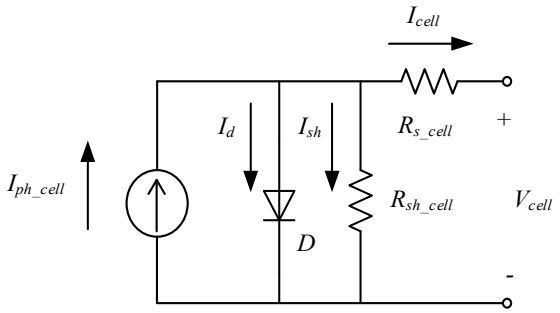

Fig. 2. Equivalent circuit of a solar cell.

The symbols in Fig.2 are defined as follows: I_{ph_cell} is the cell photocurrent, I_d is the current of the parallel diode, I_{sh} is the shunt current, I_{cell} and V_{cell} are the output current and voltage of the cell, D is the parallel diode, R_{sh_cell} is the shunt resistance, and R_{s_cell} is the series resistance. The I-V equation of the cell in Fig. 2 is shown as:

$$I_{cell} = I_{ph\_cell} - I_{o\_cell}\{e^{\frac{q(V_{cell}+R_{s\_cell}I_{cell})}{A_{cell}KT_{cell}}} - 1\} - \frac{V_{cell}+R_{s\_cell}I_{cell}}{R_{sh\_cell}} \quad (1)$$

Where I_{o_cell} is the reverse saturation current of the diode, q is the electron charge (1.602×10^{-19} C), A_{cell} is the PN junction ideal factor, K is the Boltzmann constant (1.38×10^{-23} J/K), and T_{cell} is the temperature of the cell.

In the one hand, the value of R_{sh_cell} is much greater than the value of $V_{cell}+R_{s\_cell}I_{cell}$ [13]. On the other hand, by approximating I_{ph_cell} as I_{SC_cell}, Equation (1) can be simplified by the following equation [12]:

$$I_{cell} = I_{SC\_cell} - I_{o\_cell}(e^{\frac{q(V_{cell}+R_{s\_cell}I_{cell})}{A_{cell}KT_{cell}}} - 1) \quad (2)$$

Where I_{SC_cell} is the short circuit current of a solar cell.

Equation (2) is valid for a solar cell. PV cells are connected in a series to form a PV model. According to paper [14], the I-V equation of a PV module is derived as:

$$I_{module} = I_{SC\_cell} - I_{o\_cell}(e^{\frac{q(V_{module}+N_sR_{s\_cell}I_{cell})}{N_sA_{cell}KT_{cell}}} - 1) \quad (3)$$

Where N_s is the number of series connected solar cells in a PV module.

In addition, Equation (3) can be simplified as:

$$I_{module} = I_{SC} - I_o(e^{\frac{q(V_{module}+R_sI_{module})}{AKT}} - 1) \quad (4)$$

Where I_{SC} is the short-circuit current of a PV module, I_o is the reverse saturation current of the equivalent diode of a PV module, A is the ideal factor, R_s is the series resistance, V_{module} and I_{module} are the output voltage and current of a PV module, and T is the temperature of a PV module.

According to the model in reference [13], under the STC, the model of a PV module can be obtained from Equation (4).

$$I_{module} = I_{SC}\{1\text{-}C_1(e^{\frac{V_{module}}{C_2V_{OC}}}\text{-}1)\} \quad (5)$$

$$C_1 = (1-\frac{I_M}{I_{SC}})e^{\frac{-V_M}{C_2 V_{OC}}} \quad (6)$$

$$C_2 = (\frac{V_M}{V_{OC}}-1)[\ln(1-\frac{I_M}{I_{SC}})]^{-1} \quad (7)$$

Where C_1 and C_2 are constants under the STC, V_{OC} is the open circuit voltage of the PV module under the STC, I_M and V_M are the current and voltage at the maximum power point (MPP) under the STC.

Due to the fact that most PV module manufacturers just provide the electrical specifications of PV modules under the STC, *DI* and *DV* are defined as variations of the current and voltage between the STC and the various conditions [15] shown in Equations 8 and 9.

$$DI = \alpha \frac{S}{S_{\text{ref}}}(T - T_{ref}) + (\frac{S}{S_{ref}} - 1)I_{SC} \quad (8)$$

$$DV = -\beta(T - T_{ref}) - R_s DI \quad (9)$$

Where T_{ref} is the reference temperature of a PV module under the STC, S is the in-plane irradiance, S_{ref} is the reference irradiance under the STC, α and β denote the temperature coefficients of I_{SC} and V_{OC}, respectively.

Then, the I-V equation of a PV module under various conditions can be deduced as follows:

$$I_{module} = I_{SC}\{1\text{-}C_1(e^{\frac{V_{module}\text{-}DV}{C_2 V_{OC}}}\text{-}1)\}+DI \quad (10)$$

The following sections will present the performances of PV arrays which are based on Equation (10).

B. SP Topology Analysis of a 3×2 PV ARRAY

Bypass diodes are usually embedded in PV modules during manufacturing. As shown in Fig.3, since the mismatched PV module PVM1 in a 3×2 PV array may be bypassed by a bypass diode, two operating modes of the SP topology exist.

In Fig. 3, when PVM1 is bypassed, the operating circuit of the PV array is presented in Fig. 3(a). Then, the output power of the PV array can be obtained as follows:

$$P = (I_1 + I_2)V \quad (11)$$

Where P is the output power of the PV array, I_1 is the current of the right branch formed by PVM4, PVM5 and PVM6, I_2 is the current of the left branch of PVM2 and PVM3, and V is the output voltage of the PV array. The forward voltage of the block diode and bypass diode are assumed to be V_{d}.

Since the other 5 modules work under a unique irradiance level, their characteristics are the same. Hence, the voltages of modules PVM2 and PVM3 are $(V+2V_{\text{d}})/2$, and the voltages of modules PVM4, PVM5, PVM6 are $(V+V_{\text{d}})/3$. According to Equation (10), the I_1-V equation and I_2-V equation of the two branches in Fig. 3(a) are described as:

$$I_1 = I_{SC}[1 - C_1(\mathrm{e}^{\frac{\frac{V+V_d}{3} - DV_1}{C_2 V_{OC}}} - 1)] + DI_1 \quad (12)$$

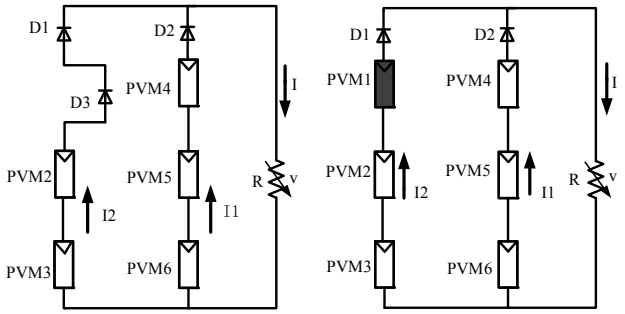

Fig. 3. Two operating circuits of SP. (a) Shaded module is by passed and (b) shaded module is not bypassed.

$$I_2 = I_{SC}[1 - C_1(\mathrm{e}^{\frac{\frac{V+2V_d}{2} - DV_1}{C_2 V_{OC}}} - 1)] + DI_1 \quad (13)$$

Where DV_1 and DI_1 are the variations of the voltage and current of a healthy PV module between the present condition and the STC, as shown in Equation (8) and (9).

In addition, the derivative of the PV array power with respect to the PV array voltage is zero at the MPP. Thus, the derivative of Equation (11) with respect to V turns to:

$$\frac{dP}{dV} = I_1 + I_2 + V(\frac{dI_1}{dV} + \frac{dI_2}{dV}) = 0 \quad (14)$$

Equation (14) is a combination of the equations of dI_1/dV, dI_2/dV and Equations (12) and (13). Therefore, a numerical solution for V can be calculated at the MPP. Finally, the output power at the MPP can be obtained.

When the operating current of PV module PVM2 or PVM3 is less than the short circuit current of PVM1, PV module PVM1 will not be bypassed and all 6 PV modules will generate power. The operating mode of the PV array is presented in Fig. 3(b).

Under these circumstances, the I_1-V equation of the right branch in Fig. 3(b) is the same as Equation (12). For the left branch, the I_2-V equation is given by:

$$\begin{aligned} V = {} & 2\{C_2 V_{OC} \ln[1 + \frac{1}{C_1}(1 - \frac{I_2 - DI_1}{I_{SC}})] + DV_1\} \\ & + C_2 V_{OC} \ln[1 + \frac{1}{C_1}(1 - \frac{I_2 - DI_2}{I_{SC}})] + DV_2 - V_d \end{aligned} \quad (15)$$

Where DV_1 and DI_1 are variations of the voltage and current of an unshaded PV module between the operating condition and the STC based on Equation (8) and (9). DV_2 and DI_2 are variations of the voltage and current of a shaded PV module between the operating condition and the STC, as shown in Equations (8) and (9).

Hence, according to Equations (12), (14), (15), dI_1/dV and dI_2/dV, the numerical solution of the output power at the MPP can be calculated in the operating mode as shown in Fig. 3(b).

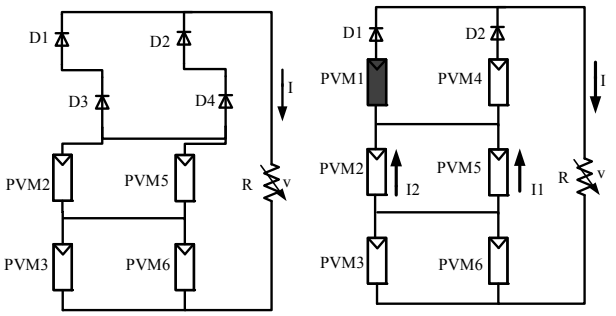

(a) (b)

Fig. 4. Two operating circuits of TCT. (a) Shaded module isn't working and (b) shaded module is working.

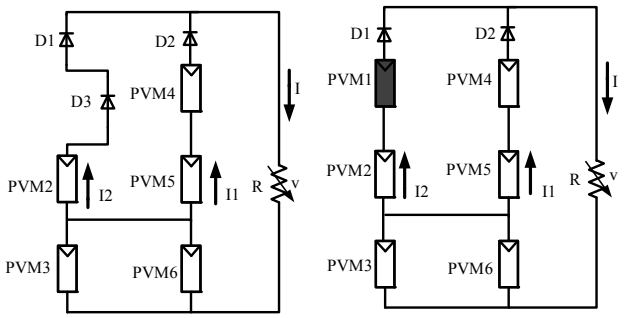

(a) (b)

Fig. 5. Two operating circuits of BL1. (a) Shaded module is bypassed and (b) shaded module is not bypassed.

C. TCT Topology Analysis of a 3×2 PV ARRAY

There are also two operating modes of the TCT topology in a 3×2 PV array when a PV module is shaded, as shown in Fig. 4.

When the sum of the short circuit currents of PV modules PVM1 and PVM4 is less than the output current of the PV array, PV module PVM1 and PVM4 will be bypassed. The operating circuit of the PV array is presented in Fig. 4(a). Then, the output power of the PV array can be obtained by:

$$P = (2V_1 - 2V_d)I \tag{16}$$

Where V_1 is the voltage of a single PV module, i.e. PVM2, PVM3, PVM5 or PVM6, I is the PV array's output current.

According to the transformation of Equation (10), V_1 can be expressed explicitly by I:

$$V_1 = C_2V_{OC}\ln[1+\frac{1}{C_1}(1-\frac{\frac{I}{2}-DI_1}{I_{SC}})]+DV_1 \tag{17}$$

Similarly, the derivative of the PV array power with respect to the PV array current is zero at the MPP, and the derivative of Equation (16) with respect to I brings:

$$\frac{dP}{dI} = 2V_1 - 2V_d + 2I\frac{dV_1}{dI} = 0 \tag{18}$$

Equation (18) is composed of dV_1/dI and Equation (17) leading to a numerical solution of I at the MPP. Therefore, the output power at the MPP can be obtained.

When the sum of the short circuit currents of PV modules PVM1 and PVM4 is greater than the output current of the PV array, all 6 PV modules will work normally. Fig. 4(b) reveals the operating circuit of the PV array under these circumstances. Then, P can be obtained by:

$$P = (2V_1 + V_2 - V_d)I \tag{19}$$

Where V_1 is the voltage of PVM2, PVM3, PVM5 or PVM6, V_2 is the voltage of PVM1 or PVM4, and I is output current of the PV array.

In this mode the I-V_1 equation in Fig. 4(b) is the same as Equation (16), and the I-V_2 equation in Fig. 4(b) is described as:

$$I = I_{SC}[1-C_1(e^{\frac{V_2-DV_1}{C_2V_{OC}}}-1)]+DI_1+I_{SC}[1-C_1(e^{\frac{V_2-DV_2}{C_2V_{OC}}}-1)]+DI_2 \tag{20}$$

Then, some terms in Equation (19) can be obtained with Equation (17) and (20). Then, it is possible to get the P-I formula of the operating circuit:

$$\begin{aligned} P = {} & I\{2C_2V_{OC}\ln[1+\frac{1}{C_1}(1-\frac{\frac{I}{2}-DI_1}{I_{SC}})]+2DV_1\} \\ & +I\{C_2V_{OC}\ln(\frac{2+\frac{2}{C_1}-\frac{I-DI_1-DI_2}{C_1I_{SC}}}{e^{\frac{-DV_1}{C_2V_{OC}}}+e^{\frac{-DV_2}{C_2V_{OC}}}})-V_d\} \end{aligned} \tag{21}$$

Due to the derivative of P in Equation (21) with respect to I being zero, the numerical solution of I and the output power can be obtained at the MPP.

D. BL1 Topology Analysis of a 3×2 PV ARRAY

As shown in Fig. 5, there are also two operating modes of the BL1 topology in a 3×2 PV array when a PV module is shaded.

When PVM1 is bypassed, the PV array's operating circuit is presented in Fig. 5(a). The voltage of PVM3 and PVM6 is denoted by V_3, and the sum of the voltages of PVM4 and PVM5 is V_4. Then, the output power can be obtained as:

$$P = (V_3 + V_4 - V_d)I \tag{22}$$

Where I is the output current of the PV array.

According to the transformation of Equation (10), the V_3-I equation in Fig. 5(a) becomes:

$$V_3 = C_2V_{OC}\ln[1+\frac{1}{C_1}(1-\frac{\frac{I}{2}-DI_1}{I_{SC}})]+DV_1 \tag{23}$$

In addition, the I-V_4 equation in Fig. 5(a) is given by:

$$\begin{aligned} I = {} & I_{SC}[1-C_1(e^{\frac{\frac{V_4}{2}-DV_1}{C_2V_{OC}}}-1)]+DI_1 \\ & +I_{SC}[1-C_1(e^{\frac{V_4-V_d-DV_1}{C_2V_{OC}}}-1)]+DI_1 \end{aligned} \tag{24}$$

Similarly, the derivative of the PV array power with respect to the PV array current is zero at the MPP. The derivative of P in Equation (22) with respect to I brings:

$$\frac{dP}{dI} = V_3 + V_4 - V_d + I(\frac{dV_3}{dI}+\frac{dV_4}{dI}) = 0 \tag{25}$$

Then terms in Equation (25) can be obtained with dV_3/dI, dV_4/dI, Equations (23) and (24), arriving at a numerical solution for V_4 at the MPP. Therefore, the output power at the MPP can be obtained in the operating circuit as shown in Fig. 5(a).

When the output current of module PVM2 is less than the short circuit current of PVM1, all 6 PV modules will generate power. The operating circuit of a PV array is presented in Fig. 5(b). Then, P can also be expressed as Equation (22), and the V_4-I_2 equation in Fig. 5(b) becomes:

$$\begin{aligned} V_4 &= C_2 V_{OC} \ln[1+\frac{1}{C_1}(1-\frac{I_2-DI_1}{I_{SC}})]+DV_1 \\ &+C_2 V_{OC} \ln[1+\frac{1}{C_1}(1-\frac{I_2-DI_2}{I_{SC}})]+DV_2 \end{aligned} \tag{26}$$

Where I_2 is the current of PVM1 and PVM2. The terms A, B and C can be set as:

$$A=\frac{1}{C_1^2 I_{SC}^2},\quad B=-(\frac{DI_1+DI_2}{C_1^2 I_{SC}^2}+\frac{2}{C_1^2 I_{SC}}+\frac{2}{C_1 I_{SC}})$$

$$C=\frac{DI_1 DI_2}{C_1^2 I_{SC}^2}+\frac{DI_1+DI_2}{C_1^2 I_{SC}}+\frac{DI_1+DI_2}{C_1 I_{SC}}+\frac{1}{C_1^2}+\frac{2}{C_1}+1-e^{\frac{V_4-DV_1-DV_2}{C_2 V_{OC}}}$$

Then, Equation (26) can be simplified to:

$$AI_2^2+BI_2+C=0 \tag{27}$$

The solution of I_2 is given by:

$$\begin{aligned} I_2 &= \frac{-B\pm\sqrt{B^2-4AC}}{2A} \\ &= C_1 I_{SC}+I_{SC}+\frac{DI_1+DI_2}{2}\pm\frac{C_1^2 I_{SC}^2}{2}\sqrt{B^2-4AC} \end{aligned} \tag{28}$$

In Equation (28), only one solution for I_2 is valid. From reference [16], the following equation can be obtained:

$$I_{SC2}=\frac{S_2}{S_{\text{ref}}}I_{SC} \tag{29}$$

In this equation, I_{SC2} and S_2 are the short circuit current and absorbed irradiance of the mismatched PV module. Generally, as the value of α in Equation (8) is very small, DI_1 and DI_2 are mainly dominated by absorbed irradiance. Therefore, by neglecting some of the terms in Equation (8), Equations (8) and (9) can be rewritten as:

$$DI_1 \approx \left(\frac{S_1}{S_{ref}}-1\right)I_{SC} \tag{30}$$

$$DI_2 \approx \left(\frac{S_2}{S_{ref}}-1\right)I_{SC} \tag{31}$$

Where S_1 is the irradiance of an unshaded PV module. I_{SC} is the short circuit current of a PV module under the STC. S_{ref} is the irradiance of a PV module under the STC.

Through Equations (29), (30) and (31), the following equation can be deduced:

$$C_1 I_{SC}+I_{SC}+\frac{DI_1+DI_2}{2}-I_{SC2}=\frac{S_1-S_2}{S_{\text{ref}}}I_{SC}>0 \tag{32}$$

That is:

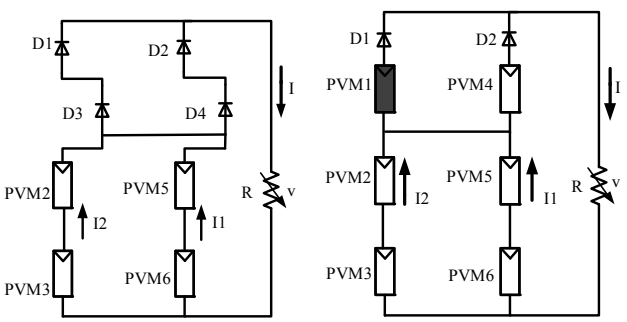

Fig. 6. Two operating modes of BL2. (a) Shaded module isn't working and (b) shaded module is working.

$$C_1 I_{SC}+I_{SC}+\frac{DI_1+DI_2}{2}>I_{SC2}\geq I_2 \tag{33}$$

Therefore, Equation (28) can be rewritten so that:

$$\begin{aligned} I_2 &= \frac{-B\pm\sqrt{B^2-4AC}}{2A} \\ &= C_1 I_{SC}+I_{SC}+\frac{DI_1+DI_2}{2}-\frac{C_1^2 I_{SC}^2}{2}\sqrt{B^2-4AC} \end{aligned} \tag{34}$$

Eventually, the output current of the PV array can be obtained by:

$$\begin{aligned} I=I_1+I_2 &= I_{SC}\left[1-C_1\left(e^{\frac{\frac{V_4}{2}-DV_1}{C_2 V_{OC}}}-1\right)\right]+DI_1 \\ &+C_1 I_{SC}+I_{SC}+\frac{DI_1+DI_2}{2}-\frac{C_1^2 I_{SC}^2}{2}\sqrt{B^2-4AC} \end{aligned} \tag{35}$$

Where I_1 is the output current of PVM4 and PVM5.

To reduce the number of variables in Equation (22), Equations (23) and (35) are substituted by (22) to get the P-V_4 equation. Based on the fact that dP/dV_4 is equal to 0 at the MPP, the output power in the operating circuit of Fig. 5(b) can be calculated.

E. BL2 Topology Analysis of a 3×2 PV ARRAY

There are two operating modes of the BL2 topology in a 3×2 PV array when module PVM1 is shaded, as shown in Fig. 6. Obviously, the working modes of the BL2 topology are similar to those of the TCT topology under the same condition for the shading distribution of the specific 3×2 PV array. Therefore, the theoretical analysis and mathematical derivation of the BL2 topology can be omitted.

F. Simulations of the GMPP Analysis in Different 3×2 PV Array Structures

By analyzing different topology structures for a 3×2 PV array and calculating the GMPP and local maximum power point (LMPP) of each PV array topology, the M-file of MATLAB codes was programed. In this paper, an EGing-50W PV module which is constituted by 36 series-connected

TABLE I
ELECTRICAL CHARACTERISTICS OF EGING-50W

Parameter	Variable	Value
Maximum power	P_{MPP}	50W
Voltage at MPP	V_{MPP}	17.98V
Current at MPP	I_{MPP}	2.77A
Short circuit current	I_{SC}	3A
Open circuit voltage	V_{OC}	22V
Temperature coefficient of I_{SC}	α	0.04%/°C
Temperature coefficient of V_{OC}	β	-0.33%/ °C

mono-crystalline cells was applied, where 2 groups of 18 cells were paralleled with a bypass diode. The electrical characteristics of the EGing-50W under the STC, provided by the manufacturer, are shown in TABLE I.

All of the PV modules are assumed to work under the STC except for PVM1, and all of the PV modules' temperatures are the same because of the thermal inertia of the PV array. The P-V curves of the different PV array topologies will have two peaks when the array works under the above mentioned conditions. The peak at the position of the lower voltage is regarded as the left peak, while the peak at the position of higher voltage is marked as the right peak. According to the mathematical derivations in Section B, C, D and E, the numerical solution of the output power of each PV array topology at the GMPP and LMPP can be calculated by changing the irradiance of PVM1 from 0 to 1000W/m^2. The corresponding output power at the GMPP and LMPP of each array structure is shown in Fig. 7.

On the one hand, with an increase in the irradiance of PVM1, the power of each PV array topology at the MPP in the right peak increases as shown in Fig. 7. On the other hand, the power of each PV array topology at the MPP in the left peak is constant, due to the shaded PV module PVM1 being bypassed by the bypass diode.

In Fig. 7, the corresponding output power at the GMPP of each PV array topology is obtained as shown in Fig. 8.

According to Fig. 7 and Fig. 8, the GMPP of each PV array topology is likely to appear at the right peak when PVM1 is slightly shaded. In addition, compared with the other topology structures, the TCT can generate greater power at the GMPP. On the other hand, when PVM1 is seriously shaded, the GMPP appears at the left peak. The SP can generate a greater power at the GMPP.

As shown in Fig. 8, the percentage of the power deviation of each PV array topology with respect to the SP at the GMPP is shown in Fig. 9.

When the GMPP appears at the left peak for each PV array structure, the greatest power of the topology SP occurs in the three topology structures. However, when the GMPP appears in the right peak of each PV array topology, the power of the TCT topology is superior. When the equivalent irradiance of the mismatched PV module is approximately 360W/m^2, the TCT interconnection achieves greater superiority than the SP interconnection.

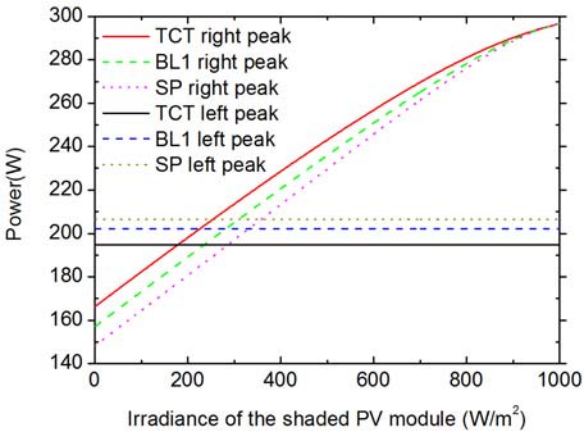

Fig. 7. Maximum power of each PV array topology structure versus the irradiance of shaded PV module.

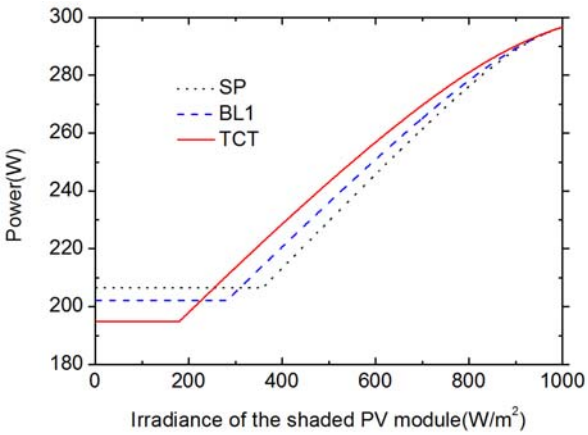

Fig. 8. Maximum power of each PV array topology structure versus the irradiance of shaded PV module.

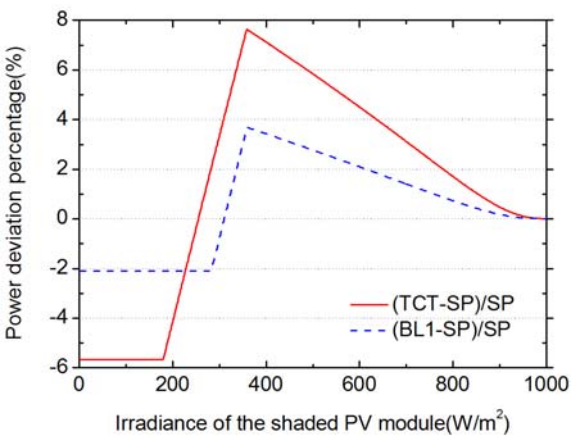

Fig. 9. The power deviation percentage at GMPP versus the irradiance of shaded PV module.

III. EXPERIMENTAL VALIDATION OF DIFFERENT INTERCONNECTIONS OF A 3×2 PV ARRAY

A. Implementation of Outdoor Experiments

To verify the proposed model for the generated power of different PV array topology structures, a flexible experimental platform was built on the rooftop of a laboratory building on campus, as shown in Fig. 10. In addition, the structure of the PV array was altered by switching the structures in Fig. 3, 4, 5 and 6. The specifications of the experimental PV modules are shown in TABLE I.

Three PV modules were mounted on a frame. A solar power meter (model: TES-1333) was used to measure the instant irradiance and a digital multimeter (model: Fluke17B) was used to measure the back sheet temperature of the PV modules. A self-designed programmable electronic load was used to measure the I-V curve after altering the structure of the PV array. The resolution of the measured voltage and current are 10 mV in a 0-90 V range and 1 mA in a 0-10 A range, respectively [17]. Finally, the I-V curves of different topology structures and their corresponding ambient parameters, i.e. irradiance and PV module temperature, are obtained simultaneously by this platform.

B. Study Cases of PV Array Interconnections under the Conditions of a Non-uniform Irradiance

Based on the platform mentioned above, the rationality of the mathematical derivation and theoretical analysis of the 3×2 PV array in Section II can be validated. In addition, the performance of different PV array topology structures under the conditions of a non-uniform irradiance can also be compared.

The conditions of a non-uniform irradiance can be simulated by using several pieces of translucent plastic to decrease the in-plane irradiance of one PV module, i.e. PV module PVM1 in Fig. 3, 4, 5 and 6. Moreover, the temperature of the PV modules can be considered to be the same due to the thermal inertia of the PV array.

Fig. 11 shows the measured P-V characteristics of the investigated 3×2 PV array with different topology structures. The irradiance level of the shaded PV module is 320W/m^2 and that of the other PV modules is 780W/m^2. The back sheet temperature of the PV modules approximates 42℃. As shown in Fig. 11, the right peak on the P-V curve of the different interconnected PV arrays is the GMPP. Compared with the other interconnection structures, the TCT and BL2 interconnections both generated greater output power. These experimental results agree with the conclusions summarized in [6], [8], [9], i.e. the TCT interconnection is the most efficient structure and can generate much more power than the SP structure when PV array mismatch occurs.

Another experiment was implemented to evaluate the different topology structures of the 3×2 PV array when the GMPP appears in the left peak of the P-V curve. The irradiance of the shaded PV module is 51W/m^2 and that of the other PV modules is 903W/m^2. Although such a low irradiance may

Fig. 10. Flexible experimental platform.

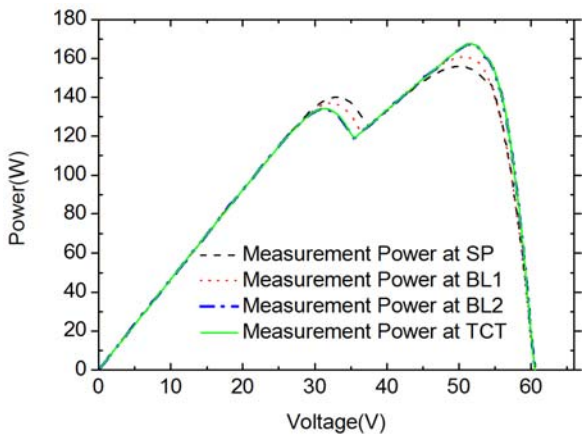

Fig. 11. Experimental P-V curves when GMPP appears at the right peak.

rarely happen in reality, some problems can be found in the experiments. The average back sheet temperature of each PV module is approximately 62℃. As shown in Fig. 12, when the mismatched PV module is severely shaded, the GMPP of the P-V curves will appear in the left peak regardless of the structure of the PV array. In fact, in a dual series connected PV array, the SP structure can generate much more power than the TCT or BL2 structure when the mismatched PV module is severely shaded. This result contradicts the conventional conclusions from other studies. This is mainly because the bypass diode of the shaded PV module conducts, which makes the PV module in the same row in a dual series connected TCT structure become bypassed. However, it does not influence the operation of the other PV modules in a SP interconnected PV array.

Fig. 11 and Fig. 12 reveal two peaks of the PV array's output power under the conditions of a non-uniform irradiance. Some conclusion can be generalized as follows:

1) Two peaks exist in a 3×2 PV array when a PV module is shaded. The GMPP may appear at the left peak or the right peak depending on the mismatch severity of the shaded PV module.
2) According to the results of the experiment, when the mismatched module is severely shaded, the superiority

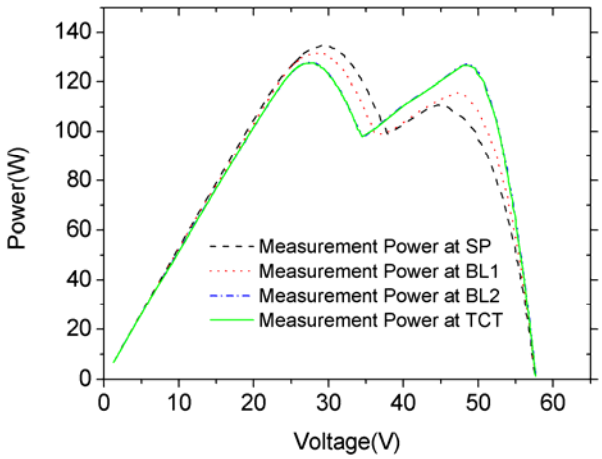

Fig. 12. Experimental P-V curves when GMPP appears at the left peak.

order of the output power of each topology structures is: SP>BL1>TCT=BL2.

3) From the results shown in Fig. 8, when the GMPP appears at the left peak, the SP interconnection has better performance than the TCT interconnection.

IV. SIMULATION ANALYSIS OF M×N PV ARRAYS

A. The extension and Analysis of N×2 PV Arrays

The output power at the GMPP or LMPP of different interconnections in a 3×2 PV array has been analyzed by deriving the relationship between the irradiance of the shaded PV module and the output power of an array. Therefore, the output power at the GMPP of a PV array that contains a different number of series-connected PV modules should be studied, such as a 5×2 or 7×2 PV array. Since the performance of the BL interconnection is between the SP and TCT for a fixed PV array, the SP and TCT topology structures are mainly discussed in this section.

Based on the derived model of the differently connected PV array in section II, the output characteristics of the SP or TCT topology structures of a 5×2 or 7×2 PV array can be obtained, as shown in Fig. 13. In this simulation, all of the PV modules are assumed to be under the STC except for the shaded PV module. The maximum power for each PV array topology structure of a 5×2 or 7×2 PV array can be calculated when the absorbed irradiance of PVM1 is increased from 0 to 1000W/m^2. Therefore, the corresponding output power at the GMPP of each topology structure versus the irradiance of the mismatched PV module can be plotted in Fig. 13.

In Fig. 13, the output power of the SP structure is greater than that of the TCT interconnection when only one PV module is severely shaded in 3×2, 5×2 and 7×2 PV arrays. On the other hand, the output power of the TCT structure is greater than that of the SP structure when the PV module is slightly shaded.

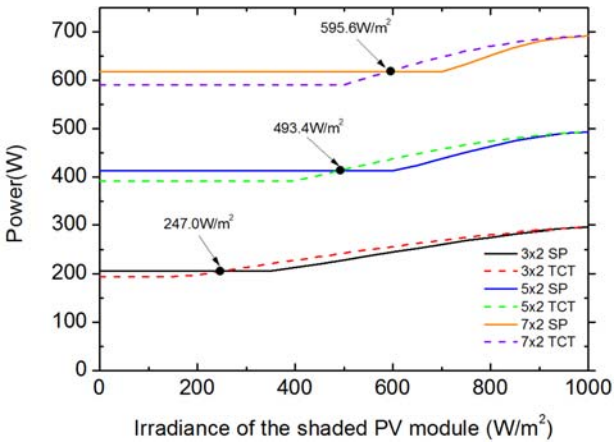

Fig. 13. Maximum power of each topology in different PV array versus the irradiance of shaded PV module.

In addition, only a critical point exists on the curves of each PV array structure, which has been marked in Fig. 13. If the equivalent irradiance of the shaded PV module can be estimated, this model can assist in switching the structure between the SP and TCT interconnections in a changeable-interconnected PV system.

Furthermore, the critical point in Fig. 13 moves towards a higher irradiance level with an increasing number of series connected PV modules in a dual series PV array. Thus, in such large scale dual series connected PV systems, the SP interconnection is recommended due to its simplicity and lower cost compared with the TCT interconnection.

B. The Simulation Analysis of More General Conditions

Considering more general conditions, 5×2 and 5×3 PV arrays are simulated when more than one module or more than one series is shaded. In this paper, in order to study the output power under more general mismatch conditions, the equivalent irradiances of the shaded PV modules are different. One of the irradiances of the two shaded PV modules is 0 to 1000 W/m^2, and the other one is 0 to 800 W/m^2. Firstly, a 5×2 PV array in different topology structures is simulated to analyze the relationship between shadow severity and output power. Fig. 15 indicates the change of the array's maximum power with the equivalent irradiance of the shaded PV module. The position of the shadow is shown in Fig. 14. Similarly, in Fig. 16 and Fig. 18, two PV modules are set to be shaded and the output powers are also analyzed with respect to the shadow severity. The results are shown in Fig. 17 and Fig. 19. Apparently, in a 5×2 PV array, the TCT can generate more power than the other structures when a slight shadow occurs. This is the same as the phenomena in a 3×2 PV array. In addition, a 5×3 PV array is also investigated. Fig. 20, Fig. 22 and Fig. 24 show the topology structures in a 5×3 PV array when one and two modules are shaded. Fig. 21, Fig. 23 and Fig. 25 are the results of the corresponding simulations. According to Fig. 23, the TCT topology can always generate greater power when two shaded modules are in the same series.

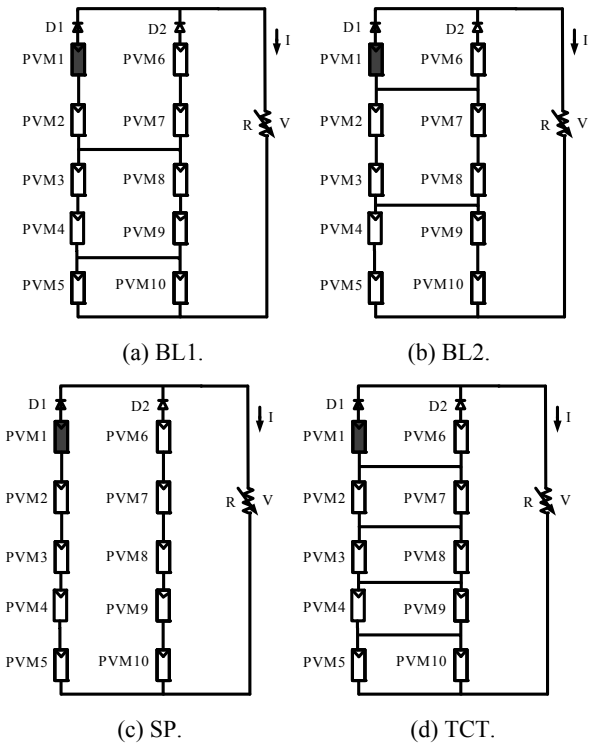

(a) BL1. (b) BL2.

(c) SP. (d) TCT.

Fig. 14. One shaded module in different topology structures in 5×2 PV array.

(a) BL1. (b) BL2.

(c) SP. (d) TCT.

Fig. 16. Two shaded module in different topology structures in 5×2 PV array.

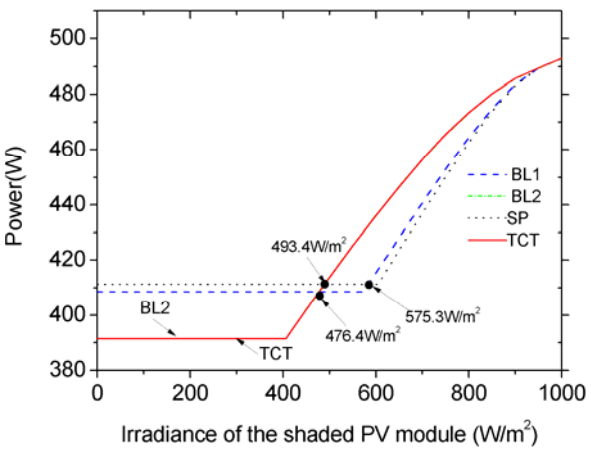

Fig. 15. Maximum power of each topology in 5×2 PV array versus the irradiance of one shaded PV module.

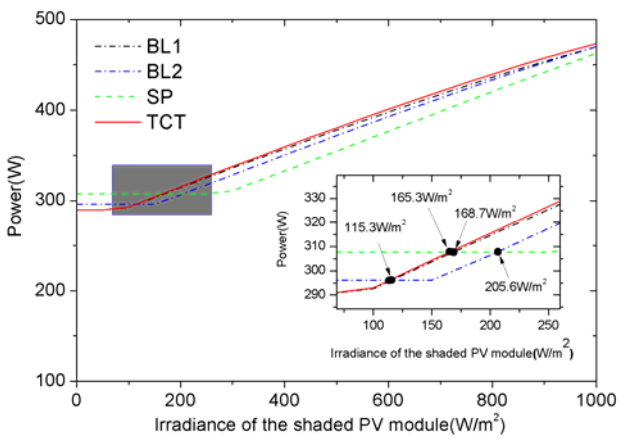

Fig. 17. Maximum power of each topology in 5×2 PV array versus the irradiance of two shaded PV modules in the same series.

This is due to the fact that the shaded PV module has not been bypassed by the bypass diodes, and the GMPP only exists at the right peak of the P-V curve.

By observing the critical points of each topology structure in Fig. 15 and Fig. 21, these critical points move towards the lower irradiance level with increments of the PV strings. When a mismatched PV module is severely shaded and bypassed, the healthy PV module is also bypassed since the operation current of the array is greater than its short-circuit current in the TCT topology structure of a 5×2 PV array. However, in a 5×3 PV array, the operation current can be shunted through other healthy PV modules in the same row as the shaded module. Therefore, they cannot be bypassed and can generate a certain amount of power.

Comparing Fig. 17 with Fig. 19, it can be seen that the output power of the SP topology structure in Fig. 19 is much greater than that in Fig. 17. If two shaded PV modules exist in the same PV string, the operation voltage of the whole array is significantly reduced due to the mismatched string. As a result, the operation point of the other healthy PV modules will be different from the individual MPP. For the whole array, this phenomenon can result in a heavier power loss. However, if two shaded PV module are in different series, as shown Fig.

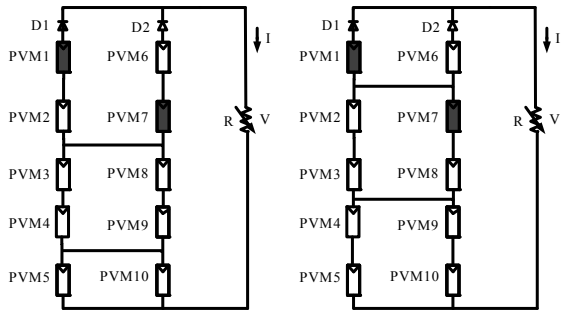

(a) BL1. (b) BL2.

(c) SP. (d) TCT.

Fig. 18. Two shaded modules in different series in 5×2 PV array.

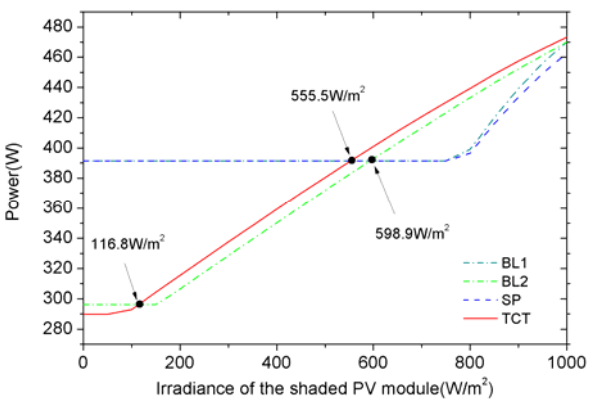

Fig. 19. Maximum power of each topology of two shaded PV modules in different series in 5×2 PV array.

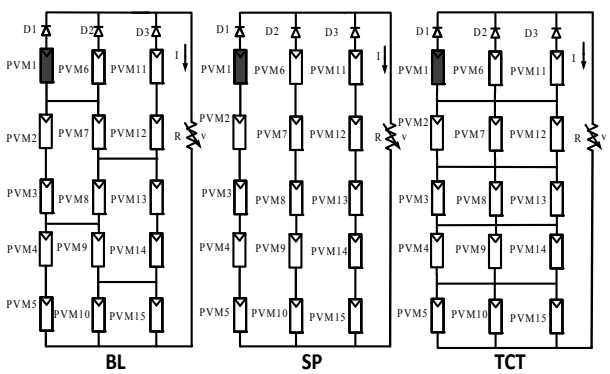

Fig. 20. One shaded module in different topology structures in 5×3 PV array.

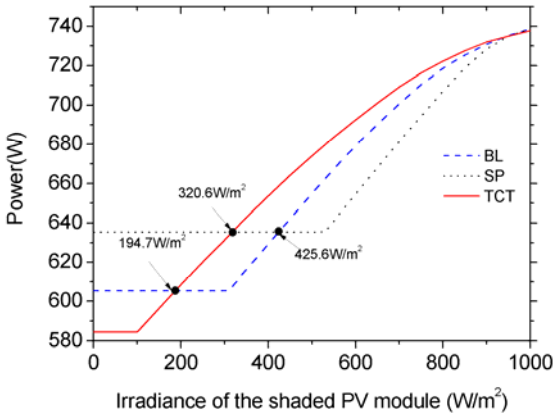

Fig. 21. Maximum power of each topology in 5×3 PV array versus the irradiance of one shaded PV module.

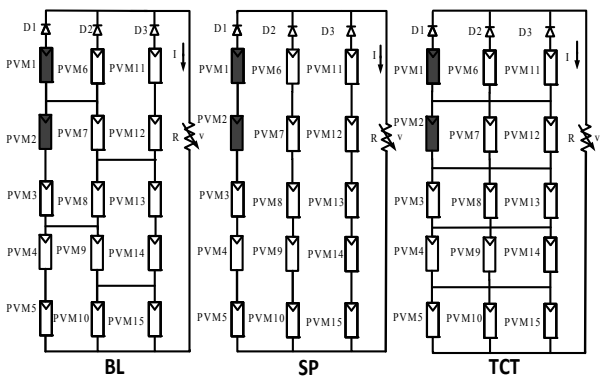

Fig. 22. Two shaded module in different topology structures in 5×3 PV array.

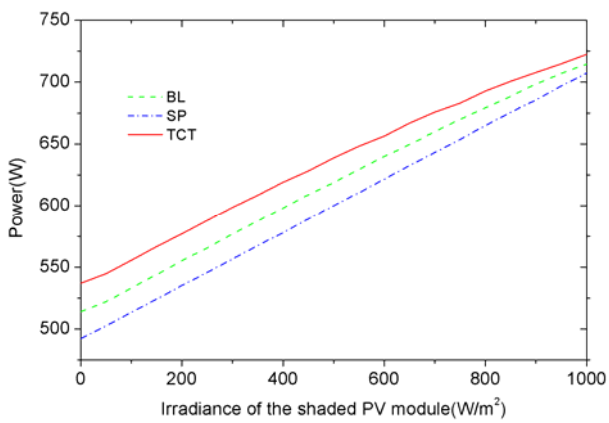

Fig. 23. Maximum power of each topology in 5×3 PV array versus the irradiance of two shaded PV modules in the same series.

18, this will cause less power loss than the situation in Fig. 16. Similarly, in Fig. 23, the GMPP only appears at the right peak of the P-V curves, and the GMPP still appears at the left peak in Fig. 25.

In general, in an M×N (M≥3, N≥2) PV array, the TCT has the highest efficiency under most conditions. The output power of the SP topology depends on the structure of the PV array

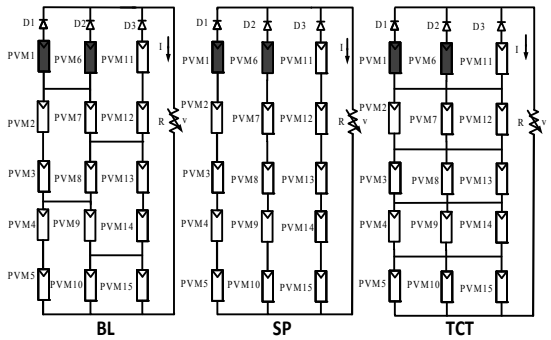

Fig. 24. Two shaded modules in different series in 5×3 PV array.

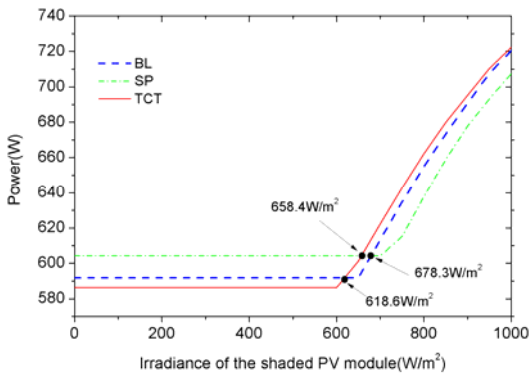

Fig. 25. Maximum power of each topology of two shaded PV modules in different series in 5×3 PV array.

and the severity of the shadow. The power generated by the BL is between the SP and the TCT.

V. CONCLUSION

Considering only one shaded PV module in a 3×2 PV array, the advantages and disadvantages of different PV array topology structures were investigated in this paper. These topology structures include the SP, BL and TCT interconnections. Based on the mathematical derivation, the output power at the GMPP or LMPP of each PV array topology structure can be obtained by increasing the irradiance of the shaded PV module from 0 to 1000 W/m^2. Then, an experimental platform was designed to validate the mathematical derivation and theoretical analysis of different topology structures in a 3×2 PV array. In addition, the SP and TCT topology structures were also studied in a 5×2 or 7×2 PV array model. Finally, the shadowing of more than one module or series were simulated. Some findings can be observed from this paper:

1. The topology structure of the SP works better than that of the TCT or BL when a mismatched PV module is severely shaded in a N×2 PV array. The topology structure of the TCT performs better than that of the SP or BL when it is slightly shaded.

2. With an increment in the number of series-connected PV modules in a N×2 PV array, the SP interconnection is more likely to perform better than that of the TCT when only one PV module is shaded.

3. According to an analysis of the output characteristics of different topology structures in 5×2 and 5×3 PV arrays, if two or more shadows are located on different series, the critical points of the SP and TCT are approximate between 500-700W/m^2. If the shadows are in the same series, the left peak becomes the only global MPP when the modules are severely shaded, and the TCT performs significantly better than the SP topology structure.

Further research will be focused on analyzing the behavior of differently structured PV arrays when two or more PV modules are shaded at the same or at different shadow levels. These circumstances are more complex than the currently built PV plants.

ACKNOWLEDGMENT

This work was supported by the Natural Science Foundation of Jiangsu Province (No. BK20131134) and State Key Laboratory of PV Science and Technology Open Foundation (No. 201400035879)，also supported by Changzhou Key Laboratory of Photovoltaic System Integration and Production Equipment Technology, Jiangsu, China.

REFERENCES

[1] F. Spertino and J. S. Akilimali, “Are manufaturing I-V mismatch and reverse currents key factors in large photovoltaic arrays,” *IEEE Trans. Ind. Electron.*, Vol. 56, No. 11, pp. 4520-4531, Nov. 2009.

[2] H. Patel and V. Agarwal, “MATLAB-based modeling to study the effects of partial shading on PV array characteristics,” *IEEE Trans. Energy Convers.*, Vol. 23, No.1, pp. 302-310, Mar. 2008.

[3] N. D. Kaushika and A. K. Rai, “An investigation of mismatch losses in solar photovoltaic cell networks,” *Energy*, Vol. 32, No.5, pp. 755-759, May 2007.

[4] A. Maki and S. Valkealahti, “Power loss in long string and parallelconnected short strings of series-connected silicon-based photovoltaic modules due to partial shading conditions,” *IEEE Trans. Energy Convers.*, Vol. 27, No. 1, pp. 173-183, Mar. 2012.

[5] N. D. Kaushika and N. K. Gautam, “Energy yield simulations of interconnected solar PV arrays,” *IEEE Trans Energy Convers.*, Vol. 18, No.1, pp. 127-134, Mar. 2003.

[6] D. Picault, B. Raison, S. Bacha, J. Aguilera, and J. Casa, “Changing photovoltaic array interconnections to reduce mismatch losses: a case study,” in *9th International Conference on Environment and Electrical Engineering (EEEIC)*, pp. 37-40, May 2010.

[7] V. Dio, D. L. Cascia, R. Miceli, and C. Rando, “A mathematical model to determine the electrical energy production in photovoltaic fields under mismatch effect,” in *International Conference on Clean Electrical Power*, pp. 46-51, Jun. 2009.

[8] N. D. Kaushika and N. K. Gautam, "Energy yield simulations of interconnected solar PV arrays," *IEEE Trans. Energy Convers.*, Vol. 18, No. 1, pp. 127-134, Mar. 2003.
[9] A. Bidram, A. Davoudi, and R. S. Balog, "Control and circuit techniques to mitigate partial shading effects in photovoltaic arrays – an overview," *IEEE J. Photovolt.*, Vol. 2, No. 4, pp. 532-546, Oct. 2012.
[10] W. D. Soto, S. A. Klein, and W. A. Beckman, "Improvement and validation of a model for photovoltaic array performance," *Solar Energy*, Vol. 80, No. 1, pp. 78-88, Jan. 2006.
[11] W. Kim and W. Choi. "A novel parameter extraction method for the one-diode solar cell model," *Solar Energy*, Vol. 84, No. 6, pp. 1008-1019, Jun. 2010.
[12] G. M. Masters, "*Renewable and efficient electric power systems*," Wiley-IEEE Press, 2004.
[13] W. D. Soto, S. A. Klein, and W. A. Beckman, "Improvement and validation of a model for photovoltaic array performance," *Solar Energy*, Vol. 80, No. 1, pp. 78-88, Jan. 2006.
[14] K. Ding, X. Bian, H. Liu, and T. Peng, "A MATLAB-simulink-based PV module model and its application under conditions of nonuniform irradiance," *IEEE Trans. Energy Conver.s*, Vol. 27, No. 4, pp. 864-872, Dec. 2012.
[15] J. Su, S. Yu, W. Zhao, M. Wu, Y. Shen, and H. He, "Investigation on engineering analytical model of silicon solar cells," *Acta Energiae Solaris Sinica*, Vol. 22, No. 4, pp. 409-412, Apr. 2001.
[16] W. Herrmann and W. Wiesner. "Current-voltage translation procedure for PV generators in german 1,000 roofs-programme," in *TUV Rheinland - EUROSUN conference,* 1996.
[17] K. Ding, J. Zhang, X. Bian, and J. Xu. "A simplified model for photovoltaic modules based on improved translation equations," *Solar Energy*, Vol. 101, pp. 40-52, Mar. 2014.

Kun Ding received his MS degree in Materials Processing Engineering and his Ph.D. degree in Electrical Engineering from Hohai University, Jiangsu, China, in 2000 and 2009, respectively. He is presently working as an Associate Professor in the College of Mechanical and Electrical Engineering, Hohai University. His current research interests include power conversion and control for renewable energy interfaces, especially photovoltaics (PV), PV array configurations, PV system designs, and dc–dc converters.

Li Feng was born in Suining, Sichuan, China. She is presently working towards her M.S. degree in the College of Mechanical and Electrical Engineering, Hohai University, Changzhou, China. Her current research interests include fault diagnosis methods and performance evaluations of distributed photovoltaic systems.

Si-Yu Qin was born in Nanning, Guangxi, China, in 1990. He received his M.S. degree in 2016 from the College of Mechanical and Electrical Engineering, Hohai University, Changzhou, China. His current research interests include the development of PV module test equipment and the analysis of the outdoor performance of PV modules.

Jing Mao received her B.S. degree from the Yangzhou University, Yangzhou, China, in 2008. In 2008 she joined Trina Solar Limited (TSL), and she is presently a Senior Engineer of the State of Key Laboratory of Photovoltaic Science at Changzhou Trina Solar Energy CO., LTD., Changzhou, China. Her current research interests include reliability assessment, failure analysis and generation analysis of PV modules and systems.

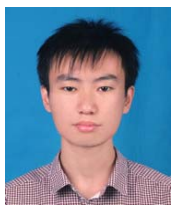

Jing-Wei Zhang was born in Nanjing, Jiangsu, China, in 1989. He is presently working towards his Ph.D. degree in the College of Energy and Electrical Engineering, Hohai University, Nanjing, China. His current research interests include the R&D of PV inverters and PV systems, power electronics and drive systems.

Xiang Wang is presently working towards his M.S. degree in the College of Mechanical and Electrical Engineering, Hohai University, Changzhou, China. His current research interests include DSP-based control and grid-connected converters for the photovoltaic (PV) modules in distributed PV systems.

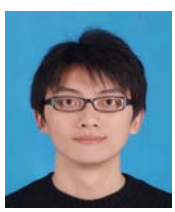

Tao Peng was born in Yancheng, Jiangsu, China, in 1988. He is presently working towards his M.S. degree in the College of Mechanical and Electrical Engineering, Hohai University, Changzhou, China. His current research interests include DSP-based control and grid-connected converters for the photovoltaic (PV) modules in distributed PV systems.

Quan-Xin Zhai is presently working towards his M.S. degree in the College of Mechanical and Electrical Engineering, Hohai University, Changzhou, China. His current research interests include DSP-based control and grid-connected converters for the photovoltaic (PV) modules in distributed PV systems.